New Journal of Physics
The open access journal at the forefront of physics

Deutsche Physikalische Gesellschaft DPG IOP Institute of Physics

OPEN ACCESS

Imaging the magnetization reversal of step-induced uniaxial magnetic anisotropy in vicinal epitaxial $La_{0.7}Sr_{0.3}MnO_3$ films

To cite this article: P Perna *et al* 2010 *New J. Phys.* **12** 103033

New Journal of Physics
The open-access journal for physics

Imaging the magnetization reversal of step-induced uniaxial magnetic anisotropy in vicinal epitaxial $La_{0.7}Sr_{0.3}MnO_3$ films

P Perna[1,2,4], L Méchin[1], M Saïb[1], J Camarero[2,3] and S Flament[1]

[1] GREYC (UMR6072) CNRS-ENSICAEN and Université de Caen Basse-Normandie, Bd de Marèchal Juin, 14050 Caen, France

[2] Instituto Madrileño de Estudios Avanzados en Nanociencia, IMDEA-Nanociencia, Campus Universidad Autónoma de Madrid, 28049 Madrid, Spain

[3] Departamento de Fisica de la Materia Condensada and Instituto 'Nicolas Cabrera', Universidad Autónoma de Madrid, 28049 Madrid, Spain

E-mail: paolo.perna@imdea.org

New Journal of Physics **12** (2010) 103033 (9pp)
Received 14 January 2010
Published 19 October 2010
Online at http://www.njp.org/
doi:10.1088/1367-2630/12/10/103033

Abstract. The magnetization reversal of $La_{0.7}Sr_{0.3}MnO_3$ (LSMO) epitaxial films deposited on 10° vicinal $SrTiO_3$(001) substrates has been investigated at room temperature by using longitudinal magneto-optical Kerr microscopy. In the case when the magnetic field is applied parallel to the substrate steps, magnetization reversal proceeds first by the nucleation of magnetic domains with well-defined magnetic domain walls (DWs) oriented parallel to the step direction and then by DW propagation. No magnetic domains are found in the case when the magnetic field is applied perpendicular to the steps, in which case magnetization reversal proceeds by coherent rotation. Our results provide a direct visualization of the step-induced uniaxial magnetic anisotropy in half-metallic systems and for LSMO thickness up to 70 nm.

The mixed-valence manganese oxides, and in particular the composition $La_{0.7}Sr_{0.3}MnO_3$ (LSMO) showing ferromagnetism up to a Curie temperature of 360 K, have attracted much interest in the condensed-matter physics community [1]–[4]. In addition to the metal–insulator transition accompanied by so-called colossal magnetoresistance (CMR) effects, they also show almost 100% spin polarization [5, 6]. Therefore, LSMO manganites appear to be potential

[4] Author to whom any correspondence should be addressed.

candidates for device applications. For instance, by using a specific pattern geometry, they could be exploited for developing magnetic field sensors [7]. Besides, spin valves based on domain wall (DW) resistivity have already been demonstrated in submicronic devices [8]–[11].

Because of the rich and complex physics related to electron–lattice and electron–electron interactions in manganites, large changes of manganite properties can be expected to take place because of lattice distortions imposed by chemical or hydrostatic pressure [12, 13] or substrate-induced strain [14]–[17]. In the case of ferromagnetic LSMO, the tensile or compressive strain induced by the film–substrate lattice mismatch can induce in-plane or out-of-plane easy magnetization directions, respectively [18]. This is commonly interpreted as because of the dominance of magnetoelastic energy over the magnetocrystalline anisotropy energy. In epitaxial LSMO thin films deposited on $SrTiO_3$ (STO) (001) surfaces, an in-plane biaxial magnetic anisotropy is generally observed, with the easy axis along the [110] and [1$\bar{1}$0] crystallographic directions [19]–[24]. The integration of half-metallic systems in real devices requires both room temperature operation and tailored magnetic anisotropy.

Artificially controlling the in-plane magnetic anisotropy in LSMO thin films by using patterned geometry and specific substrates is an exciting challenge towards single-layer active devices using spin transport properties. In particular, surface effects are one way to controllably modify the atom arrangement and the growth mode [25]. Periodic stepped substrate structures, vicinal substrates (i.e. substrates whose surface is intentionally misoriented with respect to the crystal surface) can break the fourfold rotational symmetry of the cubic structures, and a twofold magnetic anisotropy at the step edges is expected, as found in metallic magnetic materials such as Co or Fe, grown on metal or semiconductor vicinal substrates [26, 27]. Mathews *et al* [28] have reported an in-plane uniaxial magnetic anisotropy in 25- and 7-nm-thick LSMO films deposited on very low miscut STO substrates (0.13° and 0.24°) at room temperature. Wang *et al* [29] show that uniaxial magnetic anisotropy with the easy axis along the step edges could could be achieved at 80 K in 12.6-nm-thick LSMO films deposited on 10° vicinal STO substrates. A direct visualization of the magnetization reversal processes in these LSMO films as well as the answer to the question whether the step-induced uniaxial anisotropy is still effective for thicker films is still lacking. In the present work, we present magnetization reversal images of LSMO thin films epitaxially grown on vicinal STO (001) surfaces. Longitudinal magneto-optical Kerr (MOKE) microscopy measurements have been made at room temperature in two LSMO films, 16 and 70 nm thick, at different applied magnetic field angles. The evolution of the magnetic images during magnetization reversal and its angular dependence correspond to the step-induced uniaxial magnetic anisotropy scenario, with the magnetization easy axis aligned parallel to the substrate steps. This is observed for both films, i.e. for LSMO film thickness up to 70 nm.

Epitaxial LSMO thin films were deposited by pulsed laser deposition from a stoichiometric target onto commercially available low vicinal (<0.1°) STO (001) and high vicinal STO (001) substrates. In the latter case, the vicinal angle was 10° from the [001] direction towards [1$\bar{1}$0], thus inducing steps along the [110] crystallographic direction. The laser fluence was 1–2 J cm^{-2}, the target-to-substrate distance was 50 mm, the oxygen pressure was 0.35 mbar and the substrate temperature was 720 °C. Two thicknesses were chosen for LSMO films in this work, namely 16 and 70 nm. The thickness of LSMO films was obtained on the basis of x-ray reflectivity data. X-ray diffraction data show that the LSMO films grew with their (001) axis coincident with the (001) axis of the substrate, for both low and high vicinal STO substrates [30, 31].

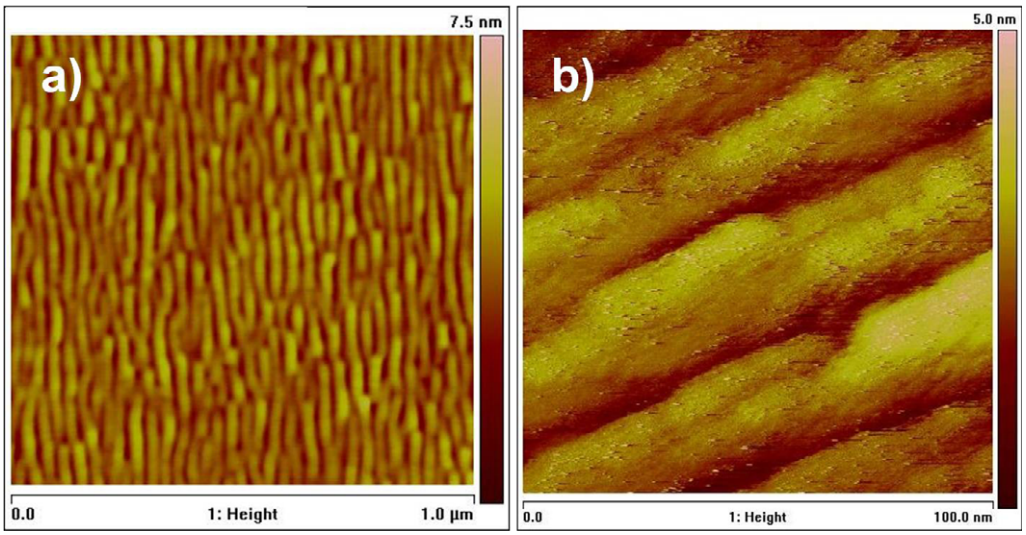

Figure 1. The surface of a 70-nm-thick LSMO film deposited on a 10° vicinal STO substrate: (a) 1 μm × 1 μm AFM image in the tapping mode; (b) 100 nm × 100 nm STM image (tunnel current = 316 pA; bias voltage = 658 mV).

Table 1. Measured magnetic parameters for the vicinal LSMO films at 300 K. M_{sat} is the saturated magnetization obtained from $M(T)$ measurements. $\mu_0 H_C$ is the coercive field, $\mu_0 H_K$ is the anisotropy field and K_u is the uniaxial magnetic anisotropy constant, measured by MOKE images as described in the text.

LSMO film thickness	M_{sat} at 10 K ($kA\,m^{-1}$)	M_{sat} at 300 K ($kA\,m^{-1}$)	$\mu_0 H_C$ at 300 K (10^{-4} T)	$\mu_0 H_K$ at 300 K (10^{-4} T)	K_u at 300 K ($J\,m^{-3}$)
16	570 ± 20	186 ± 20	2.3	14.5	135
70	590 ± 20	200 ± 20	7.9	33.0	329

Atomic force microscopy (AFM) in tapping mode and scanning tunneling microscopy (STM) were used to study the surface morphology of the films. The images of figure 1 show a very smooth LSMO surface. The root mean square (rms) roughness measured in 1 μm × 1 μm AFM images is only about 1–2 unit cells. In addition, a periodic terrace morphology oriented along the substrate step direction is observed, with an average width of 34 nm as extracted from the AFM image of a 70-nm-thick LSMO. The STM image indicates that these terraces are actually composed of several LSMO unit cells, which probably originate from step bunching during the growth. For thinner LSMO, the average terrace width is slightly larger, i.e. about 40 nm, with smaller rms.

Saturated magnetization versus temperature $M(T)$ curves were measured using a Superconducting Quantum Interference Device magnetometer [30]. An external magnetic field of 0.5 T was applied in the plane of the films, parallel and perpendicular with respect to the substrate steps. For both films, the Curie temperature T_C is 345 K and no clear difference could be observed depending on the direction of the external magnetic field. The saturated magnetization is 570 and 590 $kA\,m^{-1}$ at 10 K, and 186 and 200 $kA\,m^{-1}$ at 300 K for the 16- and 70-nm-thick films, respectively (see table 1; [30]).

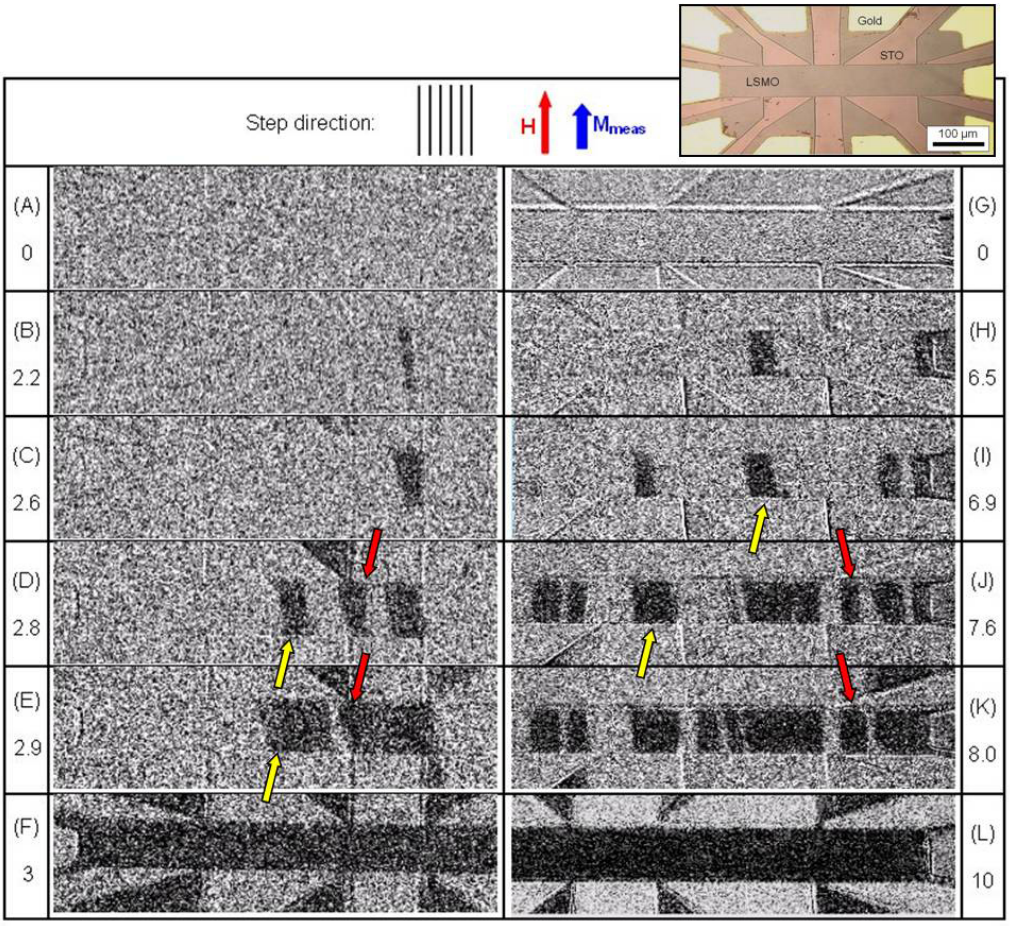

Figure 2. MOKE microscopy images showing the magnetic domain structure during magnetization reversal with H applied in the plane of the films, perpendicular to the bridge length (i.e. vertical in the images) after the films were saturated (in a magnetic field $\mu_0 H = -80 \times 10^{-4}$ T). For each image, the value of the applied magnetic field $\mu_0 H$ is indicated below each image letter and is expressed in 10^{-4} T. Images A–F and G–L were seen in the 16- and 70-nm-thick vicinal LSMO films, respectively. The steps are vertical in the images, i.e. perpendicular to the bridge length, which means that the magnetic field was applied parallel to the steps. It can be seen that magnetization reversal occurs by nucleation and propagation of the DWs in both samples. Red and orange arrows show examples of pinned DWs because of the patterned geometry and the substrate steps, respectively. In the top right inset is displayed the optical microscope photograph of a 50-μm-wide bridge patterned in the LSMO thin films.

After LSMO deposition, a 500-nm-thick gold layer was sputtered on the films in order to allow low resistive four-probe connections (which will not be detailed in this paper). The LSMO thin films were patterned by UV photolithography and argon ion etching to form 50-μm-wide bridges (see mask geometry in the insets of figures 2 and 3). A copper coil containing the sample at its center is used to apply an in-plane magnetic field perpendicular to the long

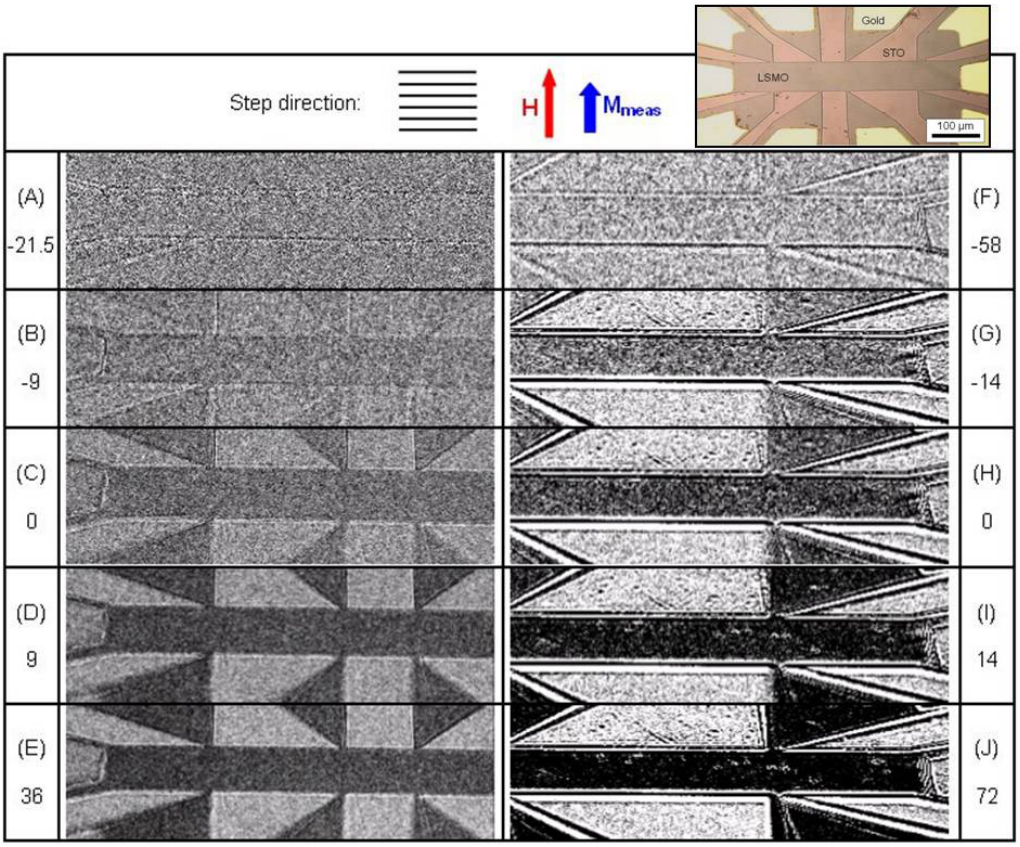

Figure 3. MOKE microscopy images showing the magnetic domain structure during magnetization reversal with H applied in the plane of the films, perpendicular to the bridge length (i.e. vertical in the images) after the films were saturated (in a magnetic field $\mu_0 H = -80 \times 10^{-4}$ T). For each image, the value of the applied magnetic field $\mu_0 H$ is indicated below each image letter and is expressed in units of 10^{-4} T. Images A–E and F–J were seen in the 16- and 70-nm-thick vicinal LSMO films, respectively. The steps are horizontal in the images, i.e. parallel to the bridge length, which means that the magnetic field was applied perpendicular to the steps. It can be seen that magnetization reversal occurs by a coherent rotation of the magnetization in both samples. In the top right inset is displayed the optical microscope photograph of a 50-μm-wide bridge patterned in the LSMO thin films.

direction of the bridge. The magnetic domain arrangement of the patterned LSMO thin films was observed using longitudinal MOKE microscopy, which was set to be sensitive to the in-plane magnetization component parallel to the applied magnetic field direction. The sample is arranged on a plane inclined at 45° with respect to the incident light. A microscope objective is used to set the magnification of the area of interest. Images were acquired using a Hamamatsu 4880-80 CCD camera that operates in a 14-bit mode. The intensity of the MOKE images was coded in gray levels. For each magnetic field value, the presented MOKE images were obtained by subtracting from the measured image a reference image acquired in the saturated state. As a result of the subtraction process, the contrast is only observed in the magnetic material. The

magnetization curves were deduced from the MOKE images by averaging the intensity over a rectangular area comprising only the LSMO rectangular bridge, which was the same for each applied field. Then, the normalized intensity values were plotted as a function of the applied magnetic field.

Figures 2 and 3 show a series of MOKE images recorded during magnetization reversal from one saturated state (light gray) to the opposite one (black) for both patterned LSMO films deposited on 10° vicinal STO (001) with the magnetic field applied either parallel (figure 2) or perpendicular (figure 3) to the substrate steps. They only show a part of the whole LSMO bridge shown in the insets. When the magnetic field is applied parallel to the substrate steps (figure 2), the magnetization switching process starts with the nucleation of magnetic domains (black) with straight DWs aligned parallel to the substrate steps. DWs then propagate to complete the magnetization reversal. This behavior corresponds to a magnetization easy-axis direction. The MOKE images show a sharp contrast with only black and light gray regions (i.e. intermediate gray level regions are not observed) for both films, which indicates the existence of only two magnetization directions, i.e. either parallel or antiparallel to the applied field direction (up or down in the images of figure 2) and hence separated by 180° DWs. In some images, one can note that some DWs are pinned, while other magnetic domains nucleate at several other places along the bridge length. Some DWs are pinned because of the patterned geometry (see, for example, the DW pointed by the red arrow in figure 2, steps (B)–(D)), but some others are pinned in the middle of the bridge, probably pinned by the substrate steps (see, for example, the DWs pointed out by the orange arrows in figure 2, steps (H)–(K)). The size of the magnetic domains is in the 10–50 μm range for both films. Complete magnetization reversal finally occurs after the depinning and propagation of 180° DWs from the steps. When the switching process is achieved, a uniform black bridge is observed.

Very different behavior was found when the magnetic field was applied perpendicular to the substrate steps for both films (figure 3). During the magnetization reversal, the magnetic contrast of the MOKE images changes uniformly and progressively from light gray to black, without any trace of nucleation of magnetic domains. This indicates that the magnetization reverses by coherent rotation, as expected for a magnetization hard axis direction. The easy and hard axis directions are orthogonal to each other, which confirms the step-induced uniaxial magnetic anisotropy in LSMO films grown on vicinal STO substrates. Our results confirm the one-dimensional micromagnetic model [32], which predicts that the magnetic domains are nucleated at the steps, acting also as pinning centers for the motion of DWs when the field is applied parallel to the steps, whereas a coherent rotation of the magnetization takes place when the field is applied perpendicular to the steps.

In order to have a more quantitative analysis of the step-induced uniaxial magnetic anisotropy, the MOKE intensities of the images averaged over the LSMO rectangular bridge area, and normalized by the measured values at the saturation states, have been extracted for each sample and magnetic field value. Figure 4 shows the corresponding hysteresis curves for the 16- and 70-nm-thick vicinal LSMO films. When the magnetic field was applied parallel to the steps, the magnetization curves show a square-like shape, revealing an easy axis along the steps. The measured coercive field values of $\mu_0 H_C$ were 2.3×10^{-4} and 7.9×10^{-4} T (with a relative width of the transition $\Delta H/H_C$ of 0.35 and 0.53) for the 16- and 70-nm-thick films, respectively (see table 1). The magnetization curves with the magnetic field applied perpendicular to the steps display low remanence and very little hysteresis, i.e. hard axis behavior. In figure 4, we superimposed the MOKE intensities obtained from the MOKE images

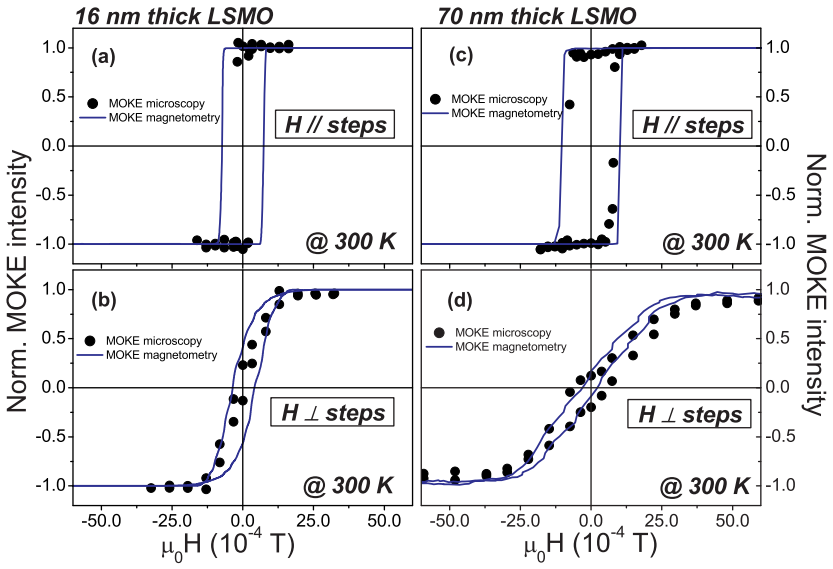

Figure 4. Normalized MOKE intensity (thus giving normalized magnetization) curves (dots) versus magnetic field applied either parallel or perpendicular to the steps measured in the 10° vicinal 16-nm-thick ((a) and (b), respectively) and 70-nm-thick ((c) and (d), respectively) LSMO films, obtained by averaging MOKE intensities over the LSMO rectangular bridge in the images of figures 2 and 3. Continuous lines (in blue) are the Kerr hysteresis loops obtained by MOKE magnetometry [29].

(dots) to the Kerr hysteresis obtained by MOKE magnetometry (lines) [30]. The agreement between the curves demonstrated that the LSMO films are not significantly influenced by the patterning geometry. Our results are in agreement with theoretical predictions based on Monte Carlo simulations [33].

The measured anisotropy field $\mu_0 H_K$ was 14.5×10^{-4} and 33×10^{-4} T for 16- and 70-nm-thick LSMO films, respectively, smaller than what was obtained for 70-nm-thick NiFe and Co films (i.e. in the range of 100–400 $\times 10^{-4}$ T) [34]. Compared with other LSMO films, our obtained results are larger than the anisotropy values found for a 25-nm-thick LSMO film grown on a low miscut angle (0.25°) vicinal STO substrate [28] and three times smaller than those found for a 12.6-nm-thick LSMO film grown on a 10° vicinal STO substrate [29]. Such a discrepancy could be interpreted in terms of the surface topography of the LSMO films, where larger anisotropy values are expected for smaller terrace widths. In our films, for a similar surface topography, we found that the anisotropy field increased as the thickness increases. The uniaxial anisotropy constants K_u at 300 K extracted from the magnetization are 135 and 329 J m^{-3} for the 16- and 70-nm-thick films, respectively (see table 1; [30]). Overall our results show that even in the 70-nm-thick LSMO film, one can observe a step-induced uniaxial magnetic anisotropy and nicely defined in-plane magnetic domain structures, which is promising for future device applications.

In summary, we have provided a direct visualization of the magnetization reversal processes in LSMO films grown on 10° vicinal STO substrates using room temperature MOKE microscopy measurements. Two different magnetization processes were seen depending on

the magnetic field direction with respect to the substrate steps. When the magnetic field is applied parallel to the steps, magnetization reversal takes place by nucleation and propagation of magnetic DWs, i.e. the easy axis, whereas a coherent rotation of the magnetization is seen when the magnetic field is applied perpendicular to the steps, i.e. the hard axis. Interestingly, the step-induced uniaxial magnetic anisotropy occurs at room temperature and for LSMO thicknesses up to 70 nm. We show that the growth of LSMO thin films on vicinal substrates offers an additional tool for magnetic domain engineering in LSMO thin films for future tailored magnetic devices.

Acknowledgments

PP acknowledges partial financial support through exchange grants from the European Science Foundation (ESF) through the activity entitled 'Thin Films for Novel Oxide Devices' (http://www.ims.tnw.utwente.nl/thiox/). We thank Ch Simon at CRISMAT (UMR6508) for SQUID magnetization measurements, CRISMAT for the use of an x-ray diffractometer and for LSMO target fabrication and C Fur at GREYC for technical assistance. This work was supported in part by the Spanish MICINN through project no. CSD2007-00010 and by the Comunidad de Madrid through project no. S2009/MAT-1726.

References

[1] Ramirez A P 1997 *J. Phys.: Condens. Matter* **9** 8171
[2] Coey J M D, Viret M and von Molnar S 1999 *Adv. Phys.* **48** 167
[3] Tokura Y and Tomiaka Y 1999 *J. Magn. Magn. Mater.* **200** 1
[4] Haghiri-Gosnet A M and Renard J P 2003 *J. Phys. D: Appl. Phys.* **36** R127
[5] Bowen M, Bibes M, Barthélémy A, Contour J-P, Anane A, Lematre Y and Fert A 2003 *Appl. Phys. Lett.* **82** 233
[6] Park J-H, Vescovo E, Kim H-J, Kwon C, Ramesh R and Venkatesan T 1998 *Nature* **392** 794
[7] Saïb M, Belmeguenai M, Méchin L, Bloyet D and Flament S 2008 *J. Appl. Phys.* **103** 113905
[8] Wolfman J, Haghiri-Gosnet A M, Raveau B, Vieu C, Cambril E, Cornette A and Launois H 2001 *J. Appl. Phys.* **89** 6955
[9] Ruotolo A, Oropallo A, Miletto Granozio F, Pepe G P, Perna P, Scotti di Uccio U and Pullini D 2007 *Appl. Phys. Lett.* **91** 132502
[10] Ruotolo A, Oropallo A, Miletto Granozio F, Perna P and Scotti di Uccio U 2006 *Appl. Phys. Lett.* **88** 252504
[11] Arnal T, Khvalkovskii A V, Bibes M, Mercey B, Lecoeur P and Haghiri-Gosnet A M 2007 *Phys. Rev.* B **75** 220409
[12] Hwang H Y, Palstra T T M, Cheong S-W and Batlogg B 1995 *Phys. Rev.* B **52** 15046
[13] Ibarra M R, Algarabel P A, Marquina C, Blasco J and Garca J 1995 *Phys. Rev. Lett.* **75** 3541
[14] Millis A J 1998 *Nature* **392** 147
[15] Millis A J, Darling T and Migliori A 1998 *J. Appl. Phys.* **83** 1588
[16] Prellier W, Lecoeur P and Mercey B 2001 *J. Phys.: Condens. Matter* **13** 915
[17] Perroni C A, Cataudella V, De Filippis G, Iadonisi G, Ramaglia VM and Ventriglia F 2003 *Phys. Rev.* B **68** 224424
[18] Perna P, Jiménez E, Terán F J, Méchin L, Camarero J and Miranda R 2010 *Mater. Res. Soc. Symp. Proc.* 1198-E01-04
[19] Tsui F, Smoak M C, Nath T K and Eom C B 2000 *Appl. Phys. Lett.* **76** 2421
[20] Steenbeck K and Hiergeist R 1999 *Appl. Phys. Lett.* **75** 1778
[21] Lecoeur P, Trouilloud P L, Xiao G, Gong G Q and Li X W 1997 *J. Appl. Phys.* **82** 3934
[22] Suzuki Y, Hwang H Y, Cheong S W and van Dover R B 1997 *Appl. Phys. Lett.* **71** 140

[23] Berndt L M, Balbarin V and Suzuki Y 2000 *Appl. Phys. Lett.* **77** 2903
[24] Ziese M, Semmelhack H C and Busch P 2002 *J. Magn. Magn. Mater.* **246** 327–34
[25] Habermeier H U 2004 *J. Electroceram.* **13** 23
[26] Jiang Q, Yang H N and Wang G C 1995 *Phys. Rev.* B **52** 14911
[27] Shiratsuchi Y, Endo Y, Yamamoto M and Bader S D 2005 *J. Appl. Phys.* **97** 10J106
[28] Mathews M, Postma F M, Lodder J C, Jansen R, Rijnders G and Blank D H 2005 *Appl. Phys. Lett.* **87** 242507
[29] Wang Z W, Cristiani G and Habermeier H U 2003 *Appl. Phys. Lett.* **82** 3731
[30] Perna P, Jimenez E, Teran F J, Méchin L, Camarero J and Miranda R 2010 arXiv:1005.0553
[31] Perna P, Méchin L, Chauvat M P, Ruterana P, Simon Ch and Scotti di Uccio U 2009 *J. Phys.: Condens. Matter* **21** 306005
[32] Hyman R A, Zangwill A and Stiles M D 1998 *Phys. Rev.* B **58** 9276
[33] Zhao D, Liu F, Huber D L and Lagally M G 2002 *J. Appl. Phys.* **91** 3150
[34] Encinas-Oropesa A and Nguyen Van Dau F 2003 *J. Magn. Magn. Mater.* **256** 301